

---

# FTA: Stealthy and Adaptive Backdoor Attack with Flexible Triggers on Federated Learning

---

Yanqi Qiao, Dazhuang Liu, Congwen Chen, Rui Wang, Kaitai Liang  
Delft University of Technology  
y.qiao, d.liu-8, r.wang-8, kaitai.liang@tudelft.nl,  
c.chen-29@student.tudelft.nl

## Abstract

Current backdoor attacks against federated learning (FL) strongly rely on universal triggers or semantic patterns, which can be easily detected and filtered by certain defense mechanisms such as norm clipping, trigger inversion and etc. In this work, we propose a novel generator-assisted backdoor attack, FTA, against FL defenses. We for the first time consider the natural stealthiness of triggers during global inference. In this method, we build a generative trigger function that can learn to manipulate the benign samples with naturally imperceptible trigger patterns (*stealthy*) and simultaneously make poisoned samples include similar hidden features of the attacker-chosen label. Moreover, our trigger generator repeatedly produces triggers for each sample (*flexibility*) in each FL iteration (*adaptivity*), allowing it to adjust to changes of hidden features between global models of different rounds. Instead of using universal and predefined triggers of existing works, we break this wall by providing three desiderate (i.e., stealthy, flexibility and adaptivity), which helps our attack avoid the presence of backdoor-related feature representations. Extensive experiments confirmed the effectiveness (above 98% attack success rate) and stealthiness of our attack compared to prior attacks on decentralized learning frameworks with eight well-studied defenses.

## 1 Introduction

Federated learning (FL) has recently provided practical performance in various real-world applications and tasks, such as prediction of oxygen requirements of symptomatic patients with COVID-19 [13], autonomous driving [32], Gboard [56] and Siri [38]. It supports collaborative training of an accurate global model by allowing multiple agents to upload local updates, such as gradients or weights, to a server without compromising local datasets. However, this decentralized paradigm unfortunately exposes FL to a security threat — backdoor attacks [4, 55, 48, 62, 25]. Existing backdoor defenses on FL possess the capability to scrutinize the anomaly of malicious model updates. However, prior attacks fail to achieve adequate stealthiness under those robust FL systems due to malicious parameter perturbations introduced by the backdoor task.

We summarize the following open problems from the existing backdoor attacks against FL<sup>1</sup>:

**P1: The abnormality of feature extraction in convolutional layers.** Existing attacks use patch-based triggers (“squares”, “stripe” and etc.) [2, 55, 62, 25] on a fixed position or semantic backdoor triggers (shared attributes within the same class) [2, 48]. Consequently, the poisoned samples are misclassified by the victim model towards the target label after backdoor training. However, we found that prior attacks manipulate the samples with universal patterns along the whole training iterations, which fails to provide enough “stealthiness” of the hidden features of the poisoned samples.

---

<sup>1</sup>Due to space limit, we review prior backdoor attacks and defenses on FL in Appendix A.1

The backdoor training with such triggers attaches extra hidden features to the backdoor patterns or revises current hidden features from the feature space in benign classes domain. This makes the latent representations of poisoned samples extracted from filters *standalone* compared to the benign counterparts. **Figure 5 (a)** intuitively illustrates the statement. Therefore, unrestricted trigger patterns can cause aberrant weight changes in the filters for backdoor patterns. This abnormality induces weight outliers which makes the backdoor attacks vulnerable to filter-wise adversarial pruning [52, 29, 51].

**P2: The abnormality of backdoor routing in fully connected layers.** Compared with the benign model, the malicious model needs to be trained on one more task, i.e. backdoor task. Specifically, in fully connected (FC) layers, the backdoor task is to establish a *new* routing [49, 10], separated from benign ones, between the independent hidden features of attacker’s universal pattern and its corresponding target label, which yields an anomaly at the parameter level. The cause of this anomaly is natural, since the output neurons for the target label must contribute to both benign and backdoor routing, which requires significant weight/bias adjustments to the neurons involved. We note that last FC layer in the current mainstream neural networks are always with a large fraction of the total number of parameters (e.g., 98% for Classic CNN, 62% in ResNet18). As mentioned in [40], the final FC layer of the malicious classifier presents significantly greater abnormality than other FC layers, with backdoor routing being seen as the secondary source of these abnormalities. Note that these abnormalities (**P1-2**) would arise in existing universal trigger designs under FL.

**P3: The perceptible trigger for inference.** Admittedly, it is not necessary to guarantee natural stealthiness of triggers on training data against FL, since its accessibility is limited to each client exclusively due to the privacy issue. However, we pay attention to the trigger stealthiness during the inference stage, in which a poisoned sample with a naturally stealthy trigger can mislead human inspection. The test input with perceptible perturbation in FL [2, 55, 62, 25] can be easily identified by an evaluator or a user who can distinguish the difference between ‘just’ an incorrect classification/prediction of the model and the purposeful wrong decision due to a backdoor in the test/use stage.

**P1-3** can fatally harm the stealthiness and effectiveness of prior attacks under robust FL systems. The stealthiness issue can be seen in two aspects (trigger/routing). For **P3**, the visible fixed triggers contain independent hidden features, and these hidden features lead to a new backdoor routing as discussed in **P1-2**. Meanwhile, the backdoor inference stage cannot perform properly because those triggers are not sufficiently hidden. For example, we recall that DBA [55], Neurotoxin [62] and 3DFed [25] use universal patterns that can be clearly filtered out by trigger inversion method such as FLIP [59]. Moreover, **P1-2** can cause weight dissimilarity between benign and backdoor routing. And this dissimilarity can be easily detected by cluster-based filtering, such as FLAME [33]. Efficiency problem is also striking for **P1-2** since extra computational budget is required to learn the new features of the poisoned data and to form the correspondent backdoor routing. In this work, we regard the problems **P1-3** as the *stealthiness* of backdoor attacks in the context of FL.

A natural question then arises: *could we eliminate the anomalies introduced by new backdoor features and routing (i.e., tackling P1-2) while making the trigger sufficiently stealthy for inference on decentralized scenario (i.e., addressing P3)?*

To provide a concrete answer, we propose a stealthy generator-assisted backdoor attack, FTA, to adaptively (per FL iteration) provide triggers in a flexible manner (per sample) on decentralized setup. FTA achieves a satisfied stealthiness by producing imperceptible triggers with a generative neural network (GAN) [18, 1] in a *flexible* way for each sample and in an *adaptive* manner during entire FL iterations. To address **P3**, our triggers should provide natural stealthiness to avoid inspection during inference. To solve **P1**, the difference of hidden features between poisoned data and benign counterparts should be minimized. Due to the imperceptibility between poisoned and benign data in latent representation, the correspondent backdoor routing will not be formed and thus **P2** is naturally addressed.

Specifically, the generator is learnt to produce triggers for each sample, which ensure similar latent features of poisoned samples to benign ones with target label (**P1**). This idea naturally reduce the abnormality of creating an extra routing for backdoor in **P2** since the latent features make poisoned data “looks like” benign ones with target label. Thus our trigger is less perceptible and more flexible than predefined patch-based ones in prior attacks (**P3**). Additionally, to make the flexible trigger robust and adaptive to the changes in global model, the generator is continuously trained across FL

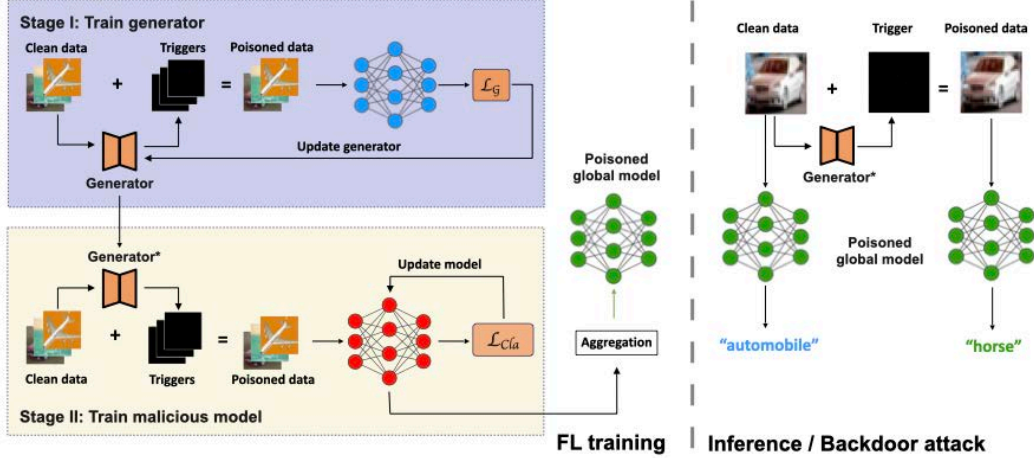


Figure 1: Overview of FTA. (I) Learn the optimal trigger generator  $g_\xi$ . (II) Train malicious model  $f_\theta$ . Inference/Backdoor Attack: The global model performs well on benign tasks while misclassifying the poisoned samples to the target label.

iterations. Compared with existing works using fixed and universal trigger patterns, we break this wall and for the first time make the generated trigger to be stealthy, flexible and adaptive in FL setups. Additionally, compared to universal trigger-based attacks, e.g., 3DFed, our trigger-assisted attack can naturally evade (universal) trigger inversion defense such as FLIP. Since our trigger generation method forces poisoned samples to share similar hidden feature as benign one, the benign routing can mostly be reused by poisoned data and thus the backdoor task is not purely learned from scratch. Our trigger generation ensures that poisoned samples have similar hidden features to benign ones, allowing poisoned data to reuse the benign routing. As a result, the backdoor task does not need to be learned entirely from scratch and achieves high attack efficiency as shown in Figure 3. Finally, we formulate the process of finding optimal trigger generator and training malicious model in a bi-level, non-convex and constrained optimization problem, and achieve optimum by proposing a simple but practical optimization process. We illustrate learning the trigger generator, training the malicious model and testing the backdoor in Figure 1, and showcase various backdoor images in Figure 2 to demonstrate the imperceptible perturbation by our generator.

Our main **contributions** are summarized as follows:

- We propose a stealthy generator-assisted backdoor attack (FTA) against robust FL. Instead of utilizing an universal trigger pattern, we design a novel trigger generator which produces naturally imperceptible triggers during inference stage. Our flexible triggers provide hidden feature similarity of benign data and successfully lead poisoned data to reuse benign routing of target label. Hereby FTA can avoid parameter anomaly of malicious update and improve attack effectiveness.
- We design a new learnable and adaptive generator that can learn the flexible triggers for global model at current FL iteration to achieve the best attack effectiveness. We propose a bi-level and constrained optimization problem to find our optimal generator each iteration efficiently. We then formulate a customized learning process for the FL scenario and solved it with reasonable complexity.
- Finally, we present intensive experiments to empirically demonstrate that the proposed attack provides state-of-the-art effectiveness and stealthiness against existing eight well-study defense mechanisms under four benchmark datasets.

## 2 Threat Model and Intuition

### 2.1 Threat Model

**Attacker’s Knowledge & Capabilities:** We consider the same threat model as in prior works [2, 4, 48, 62, 43, 36], where the attacker can have full access to malicious agent device(s), local

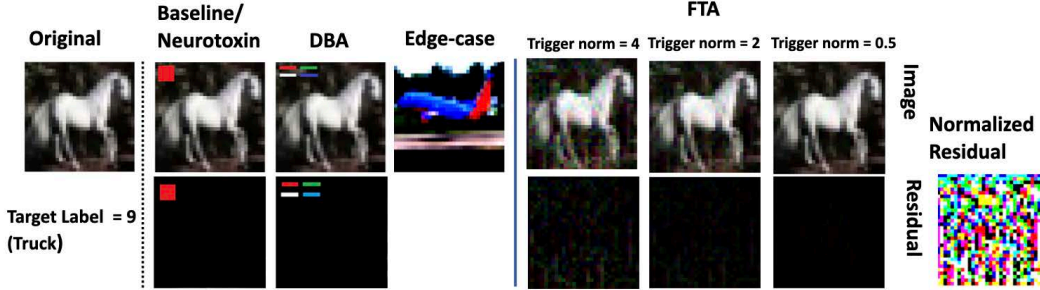


Figure 2: Visualization of backdoored images. **Top**: the original image; backdoored samples generated by baseline/Neurotoxin, DBA, Edge-case, and FTA; **Bottom**: the residual maps.

training processes and training datasets. Furthermore, we do not require the attacker to know the FL aggregation rules applied in the server.

**Attacker’s Goal:** Unlike untargeted poisoning attacks [20] preventing the convergence of the global model, the goal of our attack is to manipulate malicious agents’ local training processes to achieve high accuracy in the backdoor task without undermining the accuracy of the benign task.

## 2.2 Our Intuition

Recall that prior attacks use universal predefined patterns (see Figure 2) which cannot guarantee stealthiness (**P1-3**) since the poisoned samples are visually inconsistent with natural inputs. These universal triggers (including tail data) used in whole FL iterations with noticeable modification can introduce new hidden features during extraction and further influence the process of backdoor routing. Consequently, this makes prior attacks be easily detected by current robust defenses due to **P1-2**. Also, the inconsistency between benign and poisoned samples is not stealthy for the attacker during the global model inference (**P3**) and the triggers can be inverted in decentralized setup.

Compared to prior attacks that focus on manipulating parameters, we bridge the gap and focus on designing stealthy triggers. To address **P1-3**, a well-designed trigger should provide 4 superiorities: *i*) the poisoned sample is naturally stealthy to the original benign sample; *ii*) the trigger is able to achieve hidden feature similarity between poisoned and benign samples of target label; *iii*) the trigger can eliminate the anomaly between backdoor and benign routing during learning; *iv*) the trigger design framework can evade robust FL defenses. The only solution that provides these advantages over prior works simultaneously is *flexible* triggers. The optimal flexible triggers are learnt to make latent representations of poisoned samples similar to benign ones and thus make the reuse of benign routing possible, which naturally diminish the presence of outlier at parameter level. Therefore, to achieve the flexibility of trigger patterns and satisfy four requirements, we propose a learnable and adaptive trigger generator to produce flexible and stealthy triggers.

**v.s. Trigger generators in centralized setting.** One may argue that the attacker can simply apply a similar (trigger) generator in centralized setup [15, 14, 64, 28, 65] on FL to achieve imperceptible trigger and stealthy model update.

- **Stealthiness.** For example, the attacker can use a generator to produce imperceptible triggers for poisoned samples and make their hidden features similar to original benign samples’ as in [64, 65]. This, however, cannot ensure the indistinguishable perturbation of model parameters (caused by backdoor routing) during malicious training and fail to capture the stealthiness (in **P1-2**). This is so because it only constrains the distinction of the input domain and the hidden features between poisoned and benign samples other than the hidden features between poisoned and benign samples of **target** label. In other words, a centralized generator masks triggers in the input domain and feature space of benign samples, conceals the poisoned sample for visibility and feature representation, whereas this cannot ensure the absence of backdoor routing for poisoned data. A stealthy backdoor attack on FL should mitigate the routing introduced by backdoor task and guarantee the stealthiness of model parameters instead of just the hidden features of poisoned samples compared to their original inputs.

**Learning.** The centralized learning process of existing trigger generator cannot directly apply to decentralized setups due to the continuously changing of global model and time consumption

of training trigger generator. As an example, IBA [65] directly constrains the distance of feature representation between benign and poisoned samples. This approach cannot achieve satisfied attack effectiveness due to inaccurate hidden features of benign samples before global model convergence. In contrast, we propose a customized optimization method for FL scenarios that can learn the optimal trigger generator for global model of current iteration to achieve the best attack effectiveness and practical computational cost as depicted in Section 3.3 and Appendix A.10.

• **Defenses.** We note that the robust FL aggregator can only access local updates of all agents other than local training datasets. The centralized backdoor attack does not require consideration of the magnitude of the malicious parameters. However, in reality, the magnitude of malicious updates is usually larger than that of benign updates under FL setups. In that regard, norm clipping can effectively weaken and even eliminate the impact of the backdoor [46, 43]. Thanks to the flexibility of our triggers, we advance the state-of-the-art by enhancing the stealthiness and effectiveness of the backdoor attack even against well-studied defenses such as trigger inversion method on FL, e.g. FLIP. FLIP is effective in removing prior backdoors with patch-based triggers whereas our attack can naturally evade this SOTA defense.

### 3 Proposed Methodology: FTA

#### 3.1 Problem Formulation

Based on the federated scenario in Appendix A.1.1, the attacker  $m$  trains the malicious models to alter the behavior of the global model  $\theta$  under ERM as follows:  $\theta_m^* = \operatorname{argmin}_{\theta} \sum_{(x,y) \in D^{cln} \cup D^{bd}} \mathcal{L}(f_{\theta}(x), y)$ , where  $D^{cln}$  is clean training set and  $D^{bd}$  is a small fraction of clean samples in  $D^{cln}$  to produce poisoned data by the attacker. Each clean sample  $(x, y)$  in the selected subset is transformed into a poisoned sample as  $(\mathcal{T}(x), \eta(y))$ , where  $\mathcal{T} : \mathcal{X} \rightarrow \mathcal{X}$  is the trigger function and  $\eta$  is the target labeling function. And the poison fraction is defined as  $|D^{bd}|/|D^{cln}|$ . During inference, for a clean input  $x$  and its true label  $y$ , the learned  $f$  behaves as:  $f(x) = y, f(\mathcal{T}(x)) = \eta(y)$ .

To generate a stealthy backdoor, our main goal is to learn a stealthy trigger function  $\mathcal{T} : \mathcal{X} \rightarrow \mathcal{X}$  to craft poisoned samples and a malicious backdoor model  $f_{\theta_m^*}$  to inject backdoor behavior into the global model with the followings: 1) the poisoned sample  $\mathcal{T}(x)$  provides an imperceptible perturbation to ensure that we do not bring distribution divergences between clean and backdoor datasets; 2) the injected global classifier simultaneously performs indifferently on test input  $x$  compared to its vanilla version but changes its prediction on the poisoned image  $\mathcal{T}(x)$  to the target class  $\eta(y)$ ; 3) the latent representation of backdoor sample  $\mathcal{T}(x)$  is similar to its benign input  $x$ . Inspired by recent works in learning trigger function backdoor attacks [11, 15, 34, 64], we propose to jointly learn  $\mathcal{T}(\cdot)$  and poison  $f_{\theta}$  via the following constrained optimization:

$$\begin{aligned}
 & \min_{\theta} \sum_{(x,y) \in D^{cln}} \mathcal{L}(f_{\theta}(x), y) + \sum_{(x,y) \in D^{bd}} \mathcal{L}(f_{\theta}(\mathcal{T}_{\xi^*(\theta)}(x)), \eta(y)) \\
 s.t. \quad & (i) \quad \xi^* = \operatorname{argmin}_{\xi} \sum_{(x,y) \in D^{bd}} \mathcal{L}(f_{\theta}(\mathcal{T}_{\xi}(x)), \eta(y)) \\
 & (ii) \quad d(\mathcal{T}_{\xi}(x), x) \leq \epsilon
 \end{aligned} \tag{1}$$

where  $d$  is a distance measurement function,  $\epsilon$  is a constant scalar threshold value to ensure a small perturbation by  $l_2$ -norm constraint,  $\xi$  is the parameters of trigger function  $\mathcal{T}(\cdot)$ . In the above bilevel problem, we optimize a generative trigger function  $\mathcal{T}_{\xi^*}$  that is associated with an optimally malicious classifier. The poisoning training finds the optimal parameters  $\theta$  of the malicious classifier to minimize the linear combination of the benign and backdoor objectives. Meanwhile, the generative trigger function is trained to manipulate poisoned samples with imperceptible perturbation, while also finding the optimal trigger that can cause misclassification to the target label. The optimization in Equation (1) is a challenging task in FL scenario since the target classification model  $f_{\theta}$  varies in each iteration and its non-linear constraint. Thus, the learned trigger function  $\mathcal{T}_{\xi}$  is unstable based on dynamic  $f_{\theta}$ . For the optimization, we consider two steps: learning trigger generator and poisoning

training, and further execute these steps respectively (not alternately) to optimize  $f_\theta$  and  $\mathcal{T}_\xi$ . The details are depicted in Algorithm 1 (please see Appendix A.2 for more optimization details).

### 3.2 FTA Trigger Function

We train  $\mathcal{T}_\xi$  based on a given generative classifier  $g_\xi$ , i.e., our FTA trigger generator. Similar to the philosophy of generative trigger technology [15, 64], we design our trigger function to guarantee: 1) The perturbation of poisoned sample is imperceptible; 2) The trigger generator can learn the features of input domain of target label to fool the global model. Given a benign image  $x$  and the corresponding label  $y$ , we formally model  $\mathcal{T}_\xi$  with restricted perturbation as follows:

$$\mathcal{T}_\xi(x) = x + g_\xi(x), \quad \|g_\xi(x)\|_2 \leq \epsilon \quad \forall x, \quad \eta(y) = c, \quad (2)$$

where  $\xi$  is the learnable parameters of the FTA trigger generator and  $\epsilon$  is the trigger norm bound to constrain the value of the generative trigger norm. We use the same neural network architecture as [15] to build our trigger generator  $g_\xi$ , i.e., an autoencoder or more complex U-Net structure [41]. The  $l_2$ -norm of the imperceptible trigger noise generated by  $g_\xi$  is strictly limited within  $\epsilon$  by:  $\frac{g_\xi(x)}{\max(1, \|g_\xi(x)\|_2/\epsilon)}$ . Note that, under Equation (2), the distance  $d$  in Equation (1) is  $l_2$ -norm on the image-pixel space between  $\mathcal{T}_\xi(x)$  and  $x$ .

### 3.3 FTA's Optimization

To address the non-convex and constrained optimization in Equation (1), one may consider alternately updating  $f_\theta$  while keeping  $\mathcal{T}_\xi$  unchanged, or the other way round. However, according to our trials, we find that simply updating the parameters makes the training process unstable and harms the backdoor performance. Inspired by [16, 15], we divide the local malicious training into two phases. In phase one, we fix the classification model  $f_\theta$  and only learn the trigger function  $\mathcal{T}_\xi$ . In phase two, we use the pre-trained  $\mathcal{T}_{\xi^*}$  to generate the poisoned dataset and train the malicious classifier  $f_\theta$ . Since the number of poisoning epochs of malicious agents is fairly small, which means  $f_\theta$  would not vary too much during poisoning training process, the hidden features of samples in target label extracted from  $f_\theta$  will also remain similarly. The pre-trained  $\mathcal{T}_{\xi^*}$  can still match with the final locally trained  $f_\theta$ .

In order to make flexible triggers generated by  $g_\xi$  adaptive to global models in different rounds,  $g_\xi$  should be continuously trained. If a malicious agent is selected more than one round to participate in FL iterations, it can keep training on the previous pre-trained  $g_\xi$  under new global model to make the flexible trigger produced by  $g_\xi$  match with hidden features of benign samples with target label from new model.

---

#### Algorithm 1 FTA Backdoor Attack

---

<p><b>Input:</b> Clean dataset <math>D_{cln}</math>, Global model <math>f_\theta</math>, Learning rate of malicious model <math>\gamma_f</math> and trigger function <math>\gamma_{\mathcal{T}}</math>, Batch of clean dataset <math>B_{cln}</math> and poisoned dataset <math>B_{bd}</math>, Epochs to train trigger function <math>e_{\mathcal{T}}</math> and malicious model <math>e_f</math>.</p> <p><b>Output:</b> Malicious model update <math>\delta^*</math>.</p> <ol style="list-style-type: none"> <li>1: Initialize parameters of trigger function <math>\xi</math> and global model: <math>f_\theta</math>.</li> <li>2: Sample subset <math>D_{bd}</math> from <math>D_{cln}</math>.</li> <li>3: // <b>Stage I: Update flexible <math>\mathcal{T}</math>.</b></li> <li>4: Sample minibatch <math>(x, y) \in B_{bd}</math> from <math>D_{bd}</math></li> <li>5: <b>for</b> <math>i = 1, 2, \dots, e_{\mathcal{T}}</math> <b>do</b></li> </ol>	<ol style="list-style-type: none"> <li>6: Optimize <math>\xi</math> by using SGD with fixed <math>f_\theta</math> on <math>B_{bd}</math>: <math>\xi \leftarrow \xi - \gamma_{\mathcal{T}} \nabla_{\xi} \mathcal{L}(f_\theta(\mathcal{T}_\xi(x)), \eta(y))</math></li> <li>7: <b>end for</b></li> <li>8: <math>\xi^* \leftarrow \xi</math></li> <li>9: // <b>Stage II: Train malicious model <math>f</math>.</b></li> <li>10: Sample minibatch <math>(x, y) \in B_{cln}</math> from <math>D_{cln}</math> and <math>(x_m, y_m) \in B_{bd}</math> from <math>D_{bd}</math></li> <li>11: <b>for</b> <math>i = 1, 2, \dots, e_f</math> <b>do</b></li> <li>12: Optimize <math>\theta</math> by using SGD with fixed <math>\mathcal{T}_{\xi^*}</math> on <math>B_{cln}</math>, <math>B_{bd}</math>: <math>\theta \leftarrow \theta - \gamma_f \nabla_{\theta} (\mathcal{L}(f_\theta(x, y)) + \mathcal{L}(f_\theta(\mathcal{T}_{\xi^*}(x_m)), \eta(y_m)))</math></li> <li>13: <b>end for</b></li> <li>14: <math>\theta^* \leftarrow \theta</math></li> <li>15: Compute malicious update: <math>\delta^* \leftarrow \theta^* - \theta</math></li> </ol>
--	--

---

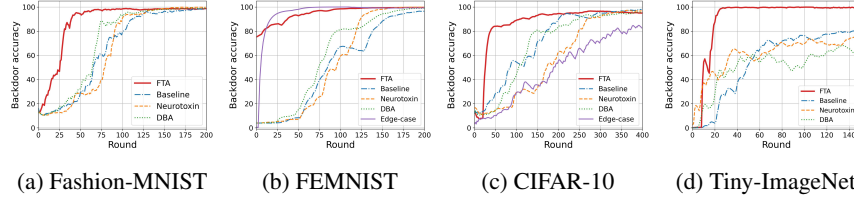


Figure 3: Fixed-frequency attack performance under FedAvg. FTA is more effective than others.

## 4 Attack Evaluation

We show that FTA outperforms the current SOTA attacks (under robust FL defenses) by conducting experiments on different computer vision tasks.

### 4.1 Experimental Setup

**Datasets and Models.** We demonstrate the effectiveness of FTA backdoor through comprehensive experiments on four publicly available datasets, namely Fashion-MNIST, FEMNIST, CIFAR-10, and Tiny-ImageNet. The classification model used in the experiments includes Classic CNN models, VGG11 [45], and ResNet18 [19]. These datasets and models are representative and commonly used in existing backdoor and FL research works. The overview of our models is described in Appendix A.6.

**Tasks.** There are 4 computer vision tasks in total using different datasets, classification models, and trigger generators respectively. The details are depicted in Appendix A.3.

**Attack Settings.** As in [62], we assume that the attacker can only compromise a limited number of agents ( $\leq 1\%$ ) in practice [43] and uses them to launch the attack by uploading manipulated gradients to the server. Malicious agents can only participate in a constrained number of training rounds in FL settings. Note even if the attacker has the above restrictions, our attack can still be effective, stealthy and robust against defenses (see Figures 3 and 4). Also, the effectiveness of the attack should last even though the attacker stops the attack under robust FL aggregators (see Figure 7 in Appendix A.4.1). We test the stealthiness and durability of FTA with two attack modes respectively, i.e., fixed-frequency and few-shot as [62].

**Fixed-frequency mode.** The server randomly chooses 10 agents among all agents. The attacker controls exactly one agent in each round in which they participate. For other rounds, 10 benign agents are randomly chosen among all agents.

**Few-shot mode.** The attacker participates only in **Attack\_num** rounds. During these rounds, we ensure that one malicious agent is selected for training. After **Attack\_num** rounds or backdoor accuracy has reached 95%, the attack will stop. Under this setting, the attack can take effect quickly, and gradually weaken by benign updates after the attack is stopped. In our experiments, the **Attack\_num** is 100 for all attacks, and the total FL round is 1000 for CIFAR-10, and 500 for other datasets.

**Evaluation Metrics.** We evaluate the performance based on backdoor accuracy (BA) and benign accuracy according to the following criteria: effectiveness and stealthiness against current SOTA defense methods under fixed-frequency mode, durability evaluated under few-shot mode.

**Comparison.** We compare FTA with three SOTA attacks, namely DBA, Neurotoxin and Edge-case [48], and the baseline attack method described in [62] under different settings and defenses. The results demonstrate that FTA delivers the best performance as compared to others.

Due to space limit, we put more experimental setup details in Appendix A.7.

### 4.2 Attack Effectiveness

**Attack effectiveness under fixed-frequency mode.** Compared to the attacks with unified triggers, FTA converges much faster and delivers the best BA in all cases, see Figure 3. It can yield a high backdoor accuracy on the server model within very few rounds ( $\leq 50$ ) and maintain above 97% accuracy on average. Especially in Tiny-ImageNet, FTA reaches 100% accuracy extremely fast,

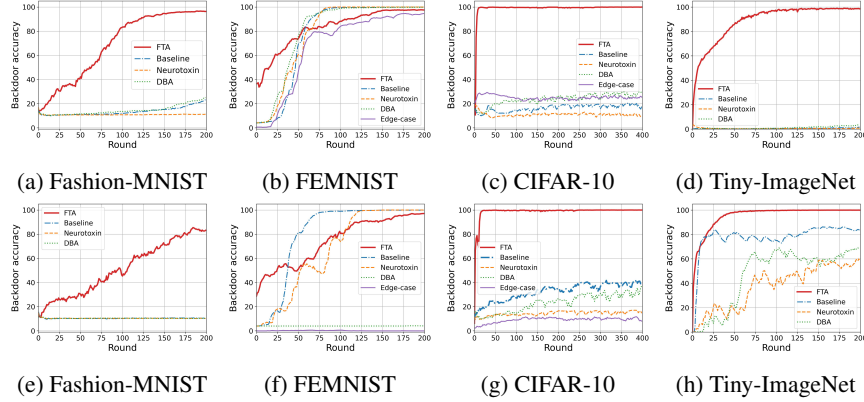


Figure 4: Attack stealthiness against defenses. (a)-(d): The variant of norm clipping; (e)-(h): FLAME.

with at least 25% advantage compared to others. In CIFAR-10, FTA achieves nearly 83% BA after 50 rounds which is 60% higher than other attacks on average. There is only  $\approx 5\%$  BA gap between FTA and Edge-case on FEMNIST in the beginning and later, they reach the same BA after 100 rounds. We note that the backdoor task of Edge-case in FEMNIST is relatively easy, mapping 7-like images to the target label of digit “1”, which makes its convergence slightly faster than ours.

**Attack effectiveness under few-shot mode.** As an independent interest, we test the durability of the attacks in this setting. Due to space limit, please see Appendix A.4.1 for more details.

**Influence on Benign accuracy and computational cost.** We include all benign accuracy results across tasks in Appendix A.5. Like other SOTA attacks, FTA has a minor effect (no more than 1.5%) on benign accuracy. Our attack does not significantly increase the computational and time cost due to our optimization procedure (see Appendix A.10 for details).

### 4.3 Stealthiness against Defensive Measures

We test the stealthiness (P1-2) and robustness of FTA and other attacks using 8 SOTA robust FL defenses introduced in Appendix A.1.3, such as norm clipping and FLAME, under fixed-frequency scenarios. All four tasks are involved in this defense evaluation. The results, see Figure 4 show that FTA can break the listed defenses. Beyond this, we also evaluate different tasks on Multi-Krum, Trimmed-mean, RFA, SignSGD, Foolsgold and SparseFed. FTA maintains its stealthiness and robustness under these defenses. We put the results of the compared attacks under the defenses in Appendix A.4.

#### 4.3.1 Resistance to Vector-wise Scaling

We use the norm clipping as the vector-wise scaling defense method, which is regarded as a potent defense and has proven effective in mitigating prior attacks [43]. On the server side, norm clipping is applied on all updates before performing FedAvg. Inspired by [33], we utilize the variant of this method in our experiments. As introduced in Appendix A.3, if we begin the attack from scratch, the norm of benign updates will be unstable and keep fluctuating, making us hard to set a fixed norm bound for all updates. We here filter out the biggest and smallest updates and compute the average norm magnitude based on the rest updates, and set it as the norm bound in current FL iteration.

As shown in Figure 4 (a)-(d), this variant of norm clipping can effectively undermine prior attacks in Fashion-MNIST, CIFAR-10, and Tiny-ImageNet. It fails in FEMNIST because benign updates have a larger norm (for example, 1.2 in FEMNIST at round 10, but only 0.3 in Fashion-MNIST), which cannot effectively clip the norm of malicious updates, thus resulting in a higher BA of existing attacks. We see that FTA provides the best BA which is less influenced by clipping than others. FTA only needs a much smaller norm to effectively fool the global model. Although converging a bit slowly in FEMNIST, FTA can finally output a similar performance (above 98%) compared to others.

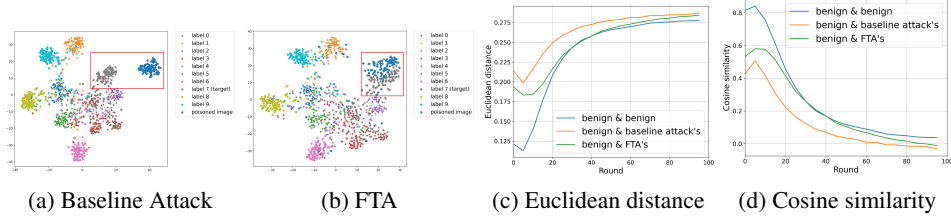


Figure 5: (a)-(b): T-SNE visualization of hidden features of input samples in Fashion-MNIST. The hidden features between poisoned and benign samples of target label is indistinguishable in FTA framework. (c)-(d): Similarity comparison between benign & malicious updates. FTA’s malicious updates is more similar to benign updates than the baseline attack’s.

### 4.3.2 Resistance to Cluster-based Filtering

The cluster-based filtering defense method is FLAME [33], which has demonstrated its effectiveness in mitigating SOTA attacks against FL. It mainly uses HDBSCAN clustering algorithm based on cosine similarity between all updates and strains the updates with the least similarity compared with other updates. In Figure 4 (e)-(h), we see that FLAME can effectively sieve malicious updates in Fashion-MNIST and CIFAR-10, but provides relatively weak effectiveness in FEMNIST and Tiny-ImageNet. This is so because data distribution among different agents are fairly in non-i.i.d. manner. Cosine similarity between benign updates is naturally low, making malicious update possibly evade from the clustering filter.

Similar to the result of Multi-Krum (see Appendix A.4.2), FTA achieves >99% BA and finishes the convergence within 50 rounds in CIFAR-10 and Tiny-ImageNet, while delivering an acceptable degradation of accuracy,  $\downarrow 20\%$ , in Fashion-MNIST. In FEMNIST, FTA converges slightly slower than the baseline and Neurotoxin but eventually maintains a similar accuracy with only 2% difference. The result proves that FTA enforces malicious updates to have highly cosine-similarity against benign updates due to the same reason in Appendix A.4.2, so that it can bypass the defenses based on similarity of updates.

## 4.4 Explanation via Feature Visualization by t-SNE

We use t-SNE [47] visualization result on CIFAR-10 to illustrate why FTA is more stealthy than the attacks without “flexible” triggers. We select 1,000 images from different classes uniformly and choose another 100 images randomly from the dataset and add triggers to them (in particular, patch-based trigger “square” in baseline method, flexible triggers in FTA). To analyze the hidden features of these samples, we use two global poisoned models injected by baseline attack and FTA respectively. We exploit the output of each sample in the last convolutional layer as the feature representation. Next, we apply dimensionality reduction techniques and cluster the latent representations of these samples using t-SNE. From Figure 5 (a)-(b), We see that in the baseline, the distance of clusters between images of the target label “7” and the poisoned images are clearly distinguishable. So the parameters responsible for backdoor routing should do adjustments to map the hidden representations of poisoned images to target label. In FTA, the hidden features of poisoned data overlapped with benign data of target label, which eliminates the anomaly in **feature extraction (P1)**. FTA can reuse the benign routing in FC layers for backdoor tasks, resulting in much less abnormality in **backdoor routing (P2)**, thus the malicious updates can be more similar to benign ones, see Figure 5 (c)-(d), producing a natural parameter stealthiness.

## 4.5 Ablation Study in FTA Attack

We here analyze several hyperparameters that are critical for the FTA’s performance.

**Trigger Size.** This size refers to the  $l_2$ -norm bound of the trigger generated by the generator, corresponding to  $\epsilon$  in Algorithm 1. If the size is set too large, the poisoned image can be easily distinguished (i.e., no stealthiness) by human inspection in test/evaluation stage. On the other hand, if we set it too small, the trigger will have a low proportion of features in the input domain. In this sense,

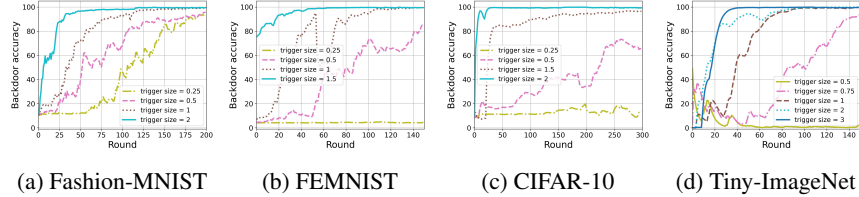


Figure 6: Different trigger sizes on backdoor accuracy.

the global model will encounter difficulty in catching and learning these features of trigger pattern, resulting in a drop of attack performance.

In Figure 6, the trigger size significantly influences the attack performance in all the tasks. The accuracies of FTA drop seriously and eventually reach closely to 0% while we keep decreasing the size of the trigger, in which evidences can be seen in CIFAR-10, FEMNIST, and Tiny-ImageNet.

The sample-specific trigger with  $l_2$ -norm bound of 2 in CIFAR-10 and Tiny-ImageNet is indistinguishable from human inspection (see Figure 12 in Appendix A.7.1), while for Fashion-MNIST and FEMNIST (images with back-and-white backgrounds), additional noise can be still easily detected. Thus, a balance between visual stealthiness and effectiveness should be considered before conducting an FTA.

**Poison Fraction.** This is the fraction of poisoned training samples in the training dataset of the attacker. Setting a low poison fraction can benefit the attack’s stealthiness by having less abnormality in parameters and less influence on benign tasks. But this can slow down the attack effectiveness, as a side effect. Fortunately, we find that FTA can still take effect under a low poison fraction. The experimental results of FTA under different poison fractions are presented in Appendix A.8.

**Dataset Size of Trigger Generator.** Theoretically, if this dataset is small-scale, the trigger generator could not be properly trained, thus resulting in bad quality and further endangering the attack performance. From Figure 13 (e)-(h) in Appendix A.8, we see that this concern should not be crucial for FTA.

#### 4.6 Natural Stealthiness

We evaluate natural stealthiness of our backdoor samples by SSIM [50] and LPIPS [60] to indicate that **P3** is well addressed by FTA flexible triggers (see Appendix A.9 for experimental results).

#### 4.7 Ablation Study in FTA Attack

We here analyze several hyperparameters that are critical for the FTA’s performance including trigger size, poison fraction and data size of our generator (please see ?? for details).

### 5 Conclusion

We design an effective and stealthy backdoor attack against FL called FTA by learning an adaptive generator to produce imperceptible and flexible triggers, making poisoned samples have similar hidden features to benign samples with target label. FTA can provide stealthiness and robustness in making hidden features of poisoned samples consistent with benign samples of target label; reducing the abnormality of parameters during backdoor task training; manipulating triggers with imperceptible perturbation for training/testing stage; learning the adaptive trigger generator across different FL rounds to generate flexible triggers with best performance. The empirical experiments demonstrate that FTA can achieve a practical performance to evade SOTA FL defenses. Due to the space limit, we present discussions on the proposed attack and experiments in Appendix A.11. We hope this work can inspire follow-up studies that provide more secure and robust FL aggregation algorithms.

## References

- [1] Martin Arjovsky, Soumith Chintala, and Léon Bottou. Wasserstein generative adversarial networks. In Doina Precup and Yee Whye Teh, editors, *Proceedings of the 34th International Conference on Machine Learning*, volume 70 of *Proceedings of Machine Learning Research*, pages 214–223. PMLR, 06–11 Aug 2017.
- [2] Eugene Bagdasaryan, Andreas Veit, Yiqing Hua, Deborah Estrin, and Vitaly Shmatikov. How to backdoor federated learning. In *International Conference on Artificial Intelligence and Statistics*, pages 2938–2948. PMLR, 2020.
- [3] Jeremy Bernstein, Jiawei Zhao, Kamyar Azizzadenesheli, and Anima Anandkumar. signsgd with majority vote is communication efficient and fault tolerant, 2019.
- [4] Arjun Nitin Bhagoji, Supriyo Chakraborty, Prateek Mittal, and Seraphin Calo. Analyzing federated learning through an adversarial lens. In *International Conference on Machine Learning*, pages 634–643. PMLR, 2019.
- [5] Peva Blanchard, El Mahdi El Mhamdi, Rachid Guerraoui, and Julien Stainer. Machine learning with adversaries: Byzantine tolerant gradient descent. *Advances in Neural Information Processing Systems*, 30, 2017.
- [6] Keith Bonawitz, Vladimir Ivanov, Ben Kreuter, Antonio Marcedone, H Brendan McMahan, Sarvar Patel, Daniel Ramage, Aaron Segal, and Karn Seth. Practical secure aggregation for federated learning on user-held data. *arXiv preprint arXiv:1611.04482*, 2016.
- [7] Sebastian Caldas, Sai Meher Karthik Duddu, Peter Wu, Tian Li, Jakub Konečný, H Brendan McMahan, Virginia Smith, and Ameet Talwalkar. Leaf: A benchmark for federated settings. *arXiv preprint arXiv:1812.01097*, 2018.
- [8] Xiaoyu Cao, Minghong Fang, Jia Liu, and Neil Gong. Fltrust: Byzantine-robust federated learning via trust bootstrapping. In *Proceedings of NDSS*, 2021.
- [9] Xiaoyu Cao, Zaixi Zhang, Jinyuan Jia, and Neil Zhenqiang Gong. Flcert: Provably secure federated learning against poisoning attacks, 2022.
- [10] Javier Carnerero-Cano, Luis Muñoz-González, Phillippa Spencer, and Emil C Lupu. Hyperparameter learning under data poisoning: Analysis of the influence of regularization via multiobjective bilevel optimization. *arXiv preprint arXiv:2306.01613*, 2023.
- [11] Siyuan Cheng, Yingqi Liu, Shiqing Ma, and Xiangyu Zhang. Deep feature space trojan attack of neural networks by controlled detoxification. In *Proceedings of the AAAI Conference on Artificial Intelligence*, volume 35, pages 1148–1156, 2021.
- [12] Yanbo Dai and Songze Li. Chameleon: Adapting to peer images for planting durable backdoors in federated learning, 2023.
- [13] Ittai Dayan, Holger R Roth, Aoxiao Zhong, Ahmed Harouni, Amilcare Gentili, Anas Z Abidin, Andrew Liu, Anthony Beardsworth Costa, Bradford J Wood, Chien-Sung Tsai, et al. Federated learning for predicting clinical outcomes in patients with covid-19. *Nature medicine*, 27(10):1735–1743, 2021.
- [14] Khoa Doan, Yingjie Lao, and Ping Li. Backdoor attack with imperceptible input and latent modification. *Advances in Neural Information Processing Systems*, 34:18944–18957, 2021.
- [15] Khoa Doan, Yingjie Lao, Weijie Zhao, and Ping Li. Lira: Learnable, imperceptible and robust backdoor attacks. In *Proceedings of the IEEE/CVF International Conference on Computer Vision*, pages 11966–11976, 2021.
- [16] Khoa D Doan, Yingjie Lao, and Ping Li. Marksman backdoor: Backdoor attacks with arbitrary target class. *arXiv preprint arXiv:2210.09194*, 2022.
- [17] Clement Fung, Chris J. M. Yoon, and Ivan Beschastnikh. The Limitations of Federated Learning in Sybil Settings. In *Symposium on Research in Attacks, Intrusion, and Defenses*, RAID, 2020.

- [18] Ian Goodfellow, Jean Pouget-Abadie, Mehdi Mirza, Bing Xu, David Warde-Farley, Sherjil Ozair, Aaron Courville, and Yoshua Bengio. Generative adversarial nets. *Advances in neural information processing systems*, 27, 2014.
- [19] Kaiming He, Xiangyu Zhang, Shaoqing Ren, and Jian Sun. Deep residual learning for image recognition. In *Proceedings of the IEEE conference on computer vision and pattern recognition*, pages 770–778, 2016.
- [20] Matthew Jagielski, Alina Oprea, Battista Biggio, Chang Liu, Cristina Nita-Rotaru, and Bo Li. Manipulating machine learning: Poisoning attacks and countermeasures for regression learning. In *2018 IEEE Symposium on Security and Privacy (SP)*, pages 19–35. IEEE, 2018.
- [21] Jing Jiang, Shaoxiong Ji, and Guodong Long. Decentralized knowledge acquisition for mobile internet applications. *World Wide Web*, 23(5):2653–2669, 2020.
- [22] Alex Krizhevsky, Geoffrey Hinton, et al. Learning multiple layers of features from tiny images. 2009.
- [23] Huseyin Kusetogullari, Amir Yavariabdi, Abbas Cheddad, Håkan Grahm, and Johan Hall. Ardis: a swedish historical handwritten digit dataset. *Neural Computing and Applications*, 32(21):16505–16518, 2020.
- [24] Ya Le and Xuan Yang. Tiny imagenet visual recognition challenge. *CS 231N*, 7(7):3, 2015.
- [25] Haoyang Li, Qingqing Ye, Haibo Hu, Jin Li, Leixia Wang, Chengfang Fang, and Jie Shi. 3dfed: Adaptive and extensible framework for covert backdoor attack in federated learning. In *2023 IEEE Symposium on Security and Privacy (SP)*, pages 1893–1907, 2023.
- [26] Tian Li, Shengyuan Hu, Ahmad Beirami, and Virginia Smith. Ditto: Fair and robust federated learning through personalization. In *International Conference on Machine Learning*, pages 6357–6368. PMLR, 2021.
- [27] Tian Li, Anit Kumar Sahu, Manzil Zaheer, Maziar Sanjabi, Ameet Talwalkar, and Virginia Smith. Federated optimization in heterogeneous networks. *Proceedings of Machine learning and systems*, 2:429–450, 2020.
- [28] Yuezun Li, Yiming Li, Baoyuan Wu, Longkang Li, Ran He, and Siwei Lyu. Invisible backdoor attack with sample-specific triggers. In *Proceedings of the IEEE/CVF International Conference on Computer Vision*, pages 16463–16472, 2021.
- [29] Kang Liu, Brendan Dolan-Gavitt, and Siddharth Garg. Fine-pruning: Defending against backdooring attacks on deep neural networks. In *International symposium on research in attacks, intrusions, and defenses*, pages 273–294. Springer, 2018.
- [30] Yang Liu, Yan Kang, Xinwei Zhang, Liping Li, Yong Cheng, Tianjian Chen, Mingyi Hong, and Qiang Yang. A communication efficient collaborative learning framework for distributed features. *arXiv preprint arXiv:1912.11187*, 2019.
- [31] Brendan McMahan, Eider Moore, Daniel Ramage, Seth Hampson, and Blaise Aguera y Arcas. Communication-efficient learning of deep networks from decentralized data. In *Artificial intelligence and statistics*, pages 1273–1282. PMLR, 2017.
- [32] Anh Nguyen, Tuong Do, Minh Tran, Binh X Nguyen, Chien Duong, Tu Phan, Erman Tjiputra, and Quang D Tran. Deep federated learning for autonomous driving. In *2022 IEEE Intelligent Vehicles Symposium (IV)*, pages 1824–1830. IEEE, 2022.
- [33] Thien Duc Nguyen, Phillip Rieger, Huili Chen, Hossein Yalame, Helen Möllering, Hossein Fereidooni, Samuel Marchal, Markus Miettinen, Azalia Mirhoseini, Shaza Zeitouni, Farinaz Koushanfar, Ahmad-Reza Sadeghi, and Thomas Schneider. FLAME: Taming backdoors in federated learning. In *31st USENIX Security Symposium (USENIX Security 22)*, pages 1415–1432, Boston, MA, August 2022. USENIX Association.
- [34] Tuan Anh Nguyen and Anh Tran. Input-aware dynamic backdoor attack. *Advances in Neural Information Processing Systems*, 33:3454–3464, 2020.

- [35] Mustafa Safa Ozdayi, Murat Kantarcioglu, and Yulia R Gel. Defending against backdoors in federated learning with robust learning rate. In *Proceedings of the AAAI Conference on Artificial Intelligence*, volume 35, pages 9268–9276, 2021.
- [36] Ashwinee Panda, Saeed Mahloujifar, Arjun Nitin Bhagoji, Supriyo Chakraborty, and Prateek Mittal. Sparsefed: Mitigating model poisoning attacks in federated learning with sparsification. In Gustau Camps-Valls, Francisco J. R. Ruiz, and Isabel Valera, editors, *Proceedings of The 25th International Conference on Artificial Intelligence and Statistics*, volume 151 of *Proceedings of Machine Learning Research*, pages 7587–7624. PMLR, 28–30 Mar 2022.
- [37] Adam Paszke, Sam Gross, Francisco Massa, Adam Lerer, James Bradbury, Gregory Chanan, Trevor Killeen, Zeming Lin, Natalia Gimelshein, Luca Antiga, et al. Pytorch: An imperative style, high-performance deep learning library. *Advances in neural information processing systems*, 32, 2019.
- [38] Matthias Paulik, Matt Seigel, Henry Mason, Dominic Telaar, Joris Kluivers, Rogier C. van Dalen, Chi Wai Lau, Luke Carlson, Filip Granqvist, Chris Vandeveld, Sudeep Agarwal, Julien Freudiger, Andrew Bye, Abhishek Bhowmick, Gaurav Kapoor, Si Beaumont, Áine Cahill, Dominic Hughes, Omid Javidbakht, Fei Dong, Rehan Rishi, and Stanley Hung. Federated evaluation and tuning for on-device personalization: System design & applications. *CoRR*, abs/2102.08503, 2021.
- [39] Krishna Pillutla, Sham M. Kakade, and Zaid Harchaoui. Robust aggregation for federated learning, 2022.
- [40] Phillip Rieger, Thien Duc Nguyen, Markus Miettinen, and Ahmad-Reza Sadeghi. Deepsight: Mitigating backdoor attacks in federated learning through deep model inspection. In *NDSS*, 2022.
- [41] Olaf Ronneberger, Philipp Fischer, and Thomas Brox. U-net: Convolutional networks for biomedical image segmentation. In *Medical Image Computing and Computer-Assisted Intervention—MICCAI 2015: 18th International Conference, Munich, Germany, October 5-9, 2015, Proceedings, Part III 18*, pages 234–241. Springer, 2015.
- [42] Virat Shejwalkar and Amir Houmansadr. Manipulating the byzantine: Optimizing model poisoning attacks and defenses for federated learning. In *NDSS*, 2021.
- [43] Virat Shejwalkar, Amir Houmansadr, Peter Kairouz, and Daniel Ramage. Back to the drawing board: A critical evaluation of poisoning attacks on production federated learning. *2022 IEEE Symposium on Security and Privacy (SP)*, pages 1354–1371, 2021.
- [44] Shiqi Shen, Shruti Tople, and Prateek Saxena. Auror: Defending against poisoning attacks in collaborative deep learning systems. In *Proceedings of the 32nd Annual Conference on Computer Security Applications, ACSAC '16*, page 508–519, New York, NY, USA, 2016. Association for Computing Machinery.
- [45] Karen Simonyan and Andrew Zisserman. Very deep convolutional networks for large-scale image recognition. In *International Conference on Learning Representations*, 2015.
- [46] Ziteng Sun, Peter Kairouz, Ananda Theertha Suresh, and H Brendan McMahan. Can you really backdoor federated learning? *arXiv preprint arXiv:1911.07963*, 2019.
- [47] Laurens Van der Maaten and Geoffrey Hinton. Visualizing data using t-sne. *Journal of machine learning research*, 9(11), 2008.
- [48] Hongyi Wang, Kartik Sreenivasan, Shashank Rajput, Harit Vishwakarma, Saurabh Agarwal, Jy-yong Sohn, Kangwook Lee, and Dimitris Papailiopoulos. Attack of the tails: Yes, you really can backdoor federated learning. *Advances in Neural Information Processing Systems*, 33:16070–16084, 2020.
- [49] Yulong Wang, Hang Su, Bo Zhang, and Xiaolin Hu. Interpret neural networks by identifying critical data routing paths. In *proceedings of the IEEE conference on computer vision and pattern recognition*, pages 8906–8914, 2018.

- [50] Zhou Wang, Alan C Bovik, Hamid R Sheikh, and Eero P Simoncelli. Image quality assessment: from error visibility to structural similarity. *IEEE transactions on image processing*, 13(4):600–612, 2004.
- [51] Chen Wu, Xian Yang, Sencun Zhu, and Prasenjit Mitra. Mitigating backdoor attacks in federated learning. *arXiv preprint arXiv:2011.01767*, 2020.
- [52] Dongxian Wu and Yisen Wang. Adversarial neuron pruning purifies backdoored deep models. *Advances in Neural Information Processing Systems*, 34:16913–16925, 2021.
- [53] Han Xiao, Kashif Rasul, and Roland Vollgraf. Fashion-mnist: a novel image dataset for benchmarking machine learning algorithms. *arXiv preprint arXiv:1708.07747*, 2017.
- [54] Chulin Xie, Minghao Chen, Pin-Yu Chen, and Bo Li. Crfl: Certifiably robust federated learning against backdoor attacks. In *International Conference on Machine Learning*, pages 11372–11382. PMLR, 2021.
- [55] Chulin Xie, Keli Huang, Pin-Yu Chen, and Bo Li. Dba: Distributed backdoor attacks against federated learning. In *International Conference on Learning Representations*, 2019.
- [56] Timothy Yang, Galen Andrew, Hubert Eichner, Haicheng Sun, Wei Li, Nicholas Kong, Daniel Ramage, and Françoise Beaufays. Applied federated learning: Improving google keyboard query suggestions, 2018.
- [57] Dong Yin, Yudong Chen, Ramchandran Kannan, and Peter Bartlett. Byzantine-robust distributed learning: Towards optimal statistical rates. In *International Conference on Machine Learning*, pages 5650–5659. PMLR, 2018.
- [58] Tao Yu, Eugene Bagdasaryan, and Vitaly Shmatikov. Salvaging federated learning by local adaptation. *arXiv preprint arXiv:2002.04758*, 2020.
- [59] Kaiyuan Zhang, Guan hong Tao, Qiuling Xu, Siyuan Cheng, Shengwei An, Yingqi Liu, Shiwei Feng, Guangyu Shen, Pin-Yu Chen, Shiqing Ma, and Xiangyu Zhang. FLIP: A provable defense framework for backdoor mitigation in federated learning. In *The Eleventh International Conference on Learning Representations*, 2023.
- [60] Richard Zhang, Phillip Isola, Alexei A Efros, Eli Shechtman, and Oliver Wang. The unreasonable effectiveness of deep features as a perceptual metric. In *Proceedings of the IEEE conference on computer vision and pattern recognition*, pages 586–595, 2018.
- [61] Zaixi Zhang, Xiaoyu Cao, and Neil Zhenqiang Gong. Fldetector: Defending federated learning against model poisoning attacks via detecting malicious clients. In *KDD*, 2022.
- [62] Zhengming Zhang, Ashwinee Panda, Linyue Song, Yaoqing Yang, Michael Mahoney, Prateek Mittal, Ramchandran Kannan, and Joseph Gonzalez. Neurotoxin: Durable backdoors in federated learning. In *Proceedings of the 39th International Conference on Machine Learning*, volume 162 of *Proceedings of Machine Learning Research*, pages 26429–26446. PMLR, 17–23 Jul 2022.
- [63] Bo Zhao, Peng Sun, Tao Wang, and Keyu Jiang. Fedinv: Byzantine-robust federated learning by inverting local model updates. In *Proceedings of the AAAI Conference on Artificial Intelligence*, volume 36, pages 9171–9179, 2022.
- [64] Zhendong Zhao, Xiaojun Chen, Yuexin Xuan, Ye Dong, Dakui Wang, and Kaitai Liang. Defeat: Deep hidden feature backdoor attacks by imperceptible perturbation and latent representation constraints. In *Proceedings of the IEEE/CVF Conference on Computer Vision and Pattern Recognition*, pages 15213–15222, 2022.
- [65] Nan Zhong, Zhenxing Qian, and Xinpeng Zhang. Imperceptible backdoor attack: From input space to feature representation. In *International Joint Conference on Artificial Intelligence*, 2022.

## A Appendix

### A.1 Related work

#### A.1.1 Federated Learning

Consider the empirical risk minimization (ERM) in FL setting where the goal is to learn a global classifier  $f_\theta : \mathcal{X} \rightarrow \mathcal{Y}$  that maps an input  $x \in \mathcal{X}$  to a target label  $y \in \mathcal{Y}$ . Recall that the FL server cannot access to training dataset. It aggregates the parameters/gradients from local agents performing centralized training with local datasets. The de-facto standard rule for aggregating the updates is so-called FedAvg [31]. The training task is to learn the global parameters  $\theta$  by solving the finite-sum optimization:  $\min_{\theta} f_\theta = \frac{1}{n} \sum_{i=1}^n f_{\theta_i}$ , where  $n$  is the number of participating agents.

At round  $t$ , the server  $S$  randomly selects  $n^t \in \{1, 2, \dots, n\}$  agents to participate in the aggregation and sends the global model  $\theta^t$  to them. Each of the agents  $i$  trains its local classifier  $f_{\theta_i} : \mathcal{X}_i \rightarrow \mathcal{Y}_i$  with its local dataset  $D_i = \{(x_j, y_j) : x_j \in \mathcal{X}_i, y_j \in \mathcal{Y}_i, j = 1, 2, \dots, N\}$  for some epochs, where  $N = |D_i|$ , by certain optimization algorithm, e.g., stochastic gradient descent (SGD). The objective of agent  $i$  is to train a local model as:  $\theta_i^* = \underset{\theta^t}{\operatorname{argmin}} \sum_{(x_j, y_j) \in D_i} \mathcal{L}(f_{\theta^t}(x_j), y_j)$ , where  $\mathcal{L}$  stands for the classification loss, e.g., cross-entropy loss. Then agent  $i$  computes its local update as  $\delta_i^t = \theta_i^* - \theta^t$ , and sends back to  $S$ . Finally, the server aggregates all updates and produces the new global model with an average  $\theta^{t+1} = \theta^t + \frac{\gamma}{|n^t|} \sum_{i \in n^t} \delta_i^t$ . where  $\gamma$  is the global learning rate. When the global model  $\theta$  converges or the training reaches a specific iteration upper bound, the aggregation process terminates and outputs a final global model. During inference, given a benign sample  $x$  and its true label  $y$ , the learned global classifier  $f_\theta$  will behave well as:  $f_\theta(x) = y$ .

Optimizations of FL have been proposed for various purposes, e.g., privacy [6], security [5, 63], heterogeneity [27], communication efficiency [30, 21] and personalization issues [26, 58].

#### A.1.2 Backdoor Attacks on FL

Current backdoor attacks can poison data and models. In data poisoning [44, 55], the attacker poisons the benign samples with a trigger pattern and marks them as a target label in order to induce the model to misbehave by training this poisoned dataset. As for model poisoning [2, 48], the attacker manipulates the training process by modifying parameters and scaling the malicious update to maximize the attack effectiveness while evading anomaly detection of robust FL aggregators [5, 46, 36, 33, 40, 57, 3].

The most well-known backdoor attack on FL is introduced in [2], where the adversary scales up the weights of malicious model updates to maximize attack impact and replace the global model with its malicious local model. To fully exploit the distributed learning methodology of FL, the local trigger patterns are used in [55] to generate poisoned images for different malicious models, while the data from the tail of the input data distribution is leveraged in [48]. Durable backdoor attacks are proposed in [62], and make attack itself more persistent in the federated scenarios. We state that this kind of attacks mainly focuses on the persistence, whereas our focus is on stealthiness.

Existing works reply on a universal trigger or tail data, which do not fully exploit the “attribute” of trigger. Our design is fully applicable and complementary to prior attacks. By learning a stealthy trigger generator and injecting the sample-specific triggers, we can significantly decrease the anomalies in **P1-3** and reinforce the stealthiness of backdoor attacks.

#### A.1.3 Backdoor Defenses on FL

There are a number of defenses that provide empirical robustness against backdoor attacks.

**Dimension-wise filtering.** Trimmed-mean [57] aggregates each dimension of model updates of all agents independently. It sorts the parameters of the  $j^{th}$ -dimension of all updates and removes  $m$  of the largest and smallest parameters in that dimension. Finally, it computes the arithmetic mean of the rest parameters as the aggregate of dimension  $j$ . Similarly, Median [57] takes the arithmetic median value of each dimension for aggregation. SignSGD [3] only aggregates the signs of the gradients (of all agents) and returns the sign to agents for updating the local models.

**Vector-wise scaling.** Norm clipping [46] bounds the  $l_2$ -norm of all updates to a fixed threshold due to high norms of malicious updates. For a threshold  $\tau$  and an update  $\nabla$ , if the norm of the update  $\|\nabla\| > \tau$ ,  $\nabla$  is scaled by  $\frac{\tau}{\|\nabla\|}$ . The server averages all the updates, scaled or not, for aggregation.

**Vector-wise filtering.** Krum [5] selects a local model, with the smallest Euclidean distance to  $n - f - 1$  of other local models, as the global model. A variant of Krum called Multi-Krum [5] selects a local model using Krum and removes it from the remaining models repeatedly. The selected model is added to a selection  $S$  until  $S$  has  $c$  models such that  $n - c > 2m + 2$ , where  $n$  is the number of selected models and  $m$  is the number of malicious models. Finally, Multi-Krum averages the selected model updates. RFA [39] aggregates model updates and makes FedAvg robust to outliers by replacing the averaging aggregation with an approximate geometric median.

**Certification.** CRFL [54] provides certified robustness in FL frameworks. It exploits parameter clipping and perturbing during federated averaging aggregation. In the test stage, it constructs a “smoothed” classifier using parameter smoothing. The robust accuracy of each test sample can be certified by this classifier when the number of compromised clients or perturbation to the test input is below a certified threshold.

**Sparsification.** SparseFed [36] performs norm clipping to all local updates and averages the updates as the aggregate.  $Top_k$  values of the aggregation update are extracted and returned to each agent who locally updates the models using this sparse update.

**Cluster-based filtering.** Recently, [33] proposed a defending framework FLAME based on the clustering algorithm (HDBSCAN) which can cluster dynamically all local updates based on their cosine distance into two groups separately. FLAME uses weight clipping for scaling-up malicious weights and noise addition for smoothing the boundary of clustering after filtering malicious updates. By using HDBSCAN, [40] designed a robust FL aggregation rule called DeepSight. Their design leverages the distribution of labels for the output layer, output of random inputs, and cosine similarity of updates to cluster all agents’ updates and further applies the clipping method.

## A.2 The procedure of FTA optimization

In case of collusion between more than one malicious agent device, the local datasets owned by these devices are in non-i.i.d. manner. Their local trigger generators  $g_{\xi_i}$  are trained by these local datasets. This kind of dataset bias can degrade attack effectiveness since their malicious updates are for local triggers from different  $g_{\xi_i}$  and cannot be merged together to yield a better attack performance. To resolve this problem, we develop a practical solution. Before starting the FTA backdoor attack, the malicious agents can share a portion of their local datasets to form a universal poisoned dataset (for all the malicious agents), so that their local generators  $g_{\xi_i}$  can produce the same triggers.

## A.3 Details of the tasks

The details of 4 computer vision tasks are described in Table 1. To prove the stealthiness and further robustness against defenses of FTA, we use a decentralized setting with non-i.i.d. data distribution among all agents. The attacker chooses the all-to-one type of backdoor attack (except Edge-case [48]), fooling the global model to misclassify the poisoned images of any label to an attacker-chosen target label. Following a practical scenario for the attacker given in [62], 10 agents among thousands of agents are selected for training in each round and their updates are used for aggregation and updating the server model. We apply backdoor attacks from different phases of training. In FEMNIST task, we follow the same setting as [55], where the attacker begins to attack when the benign accuracy of global models starts to converge. For other tasks, we perform backdoor attacks at the beginning of FL training. In this sense, as mentioned in [55], benign updates are more likely to share common patterns of gradients and have a larger magnitude than malicious updates, which can significantly restrict the effectiveness of malicious updates. Note we consider such a setting for the bottom performance of attacks and further, we still see that our attack performs more effectively than prior works in this case (see Figure 3).

Table 1: The datasets, and their corresponding models and hyperparameters.

	Fahion-MNIST	FEMNIST	CIFAR-10	Tiny-ImageNet
Classes	62	10	10	200
Size of training set	60000	737837	50000	100000
Size of testing set	10000	80014	10000	10000
Total agents	2000	3000	1000	2000
Malicious agents	2	3	1	2
Agents per FL round	10	10	10	10
Phase to start attack	Attack from scratch	Attack after convergence	Attack from scratch	Attack from scratch
Poison fraction	0.2			
Trigger size	2	1.5	1.5	3
Dataset size of trigger generator	1024			
Epochs of benign task	2	4	5	5
Epochs of backdoor task	5	10	10	10
Learning rate of trigger generator	0.01	0.01	0.001	0.01
Epochs of trigger generator	20	20	30	30
Local data distribution	non-i.i.d.			
Classification model	Classic CNN	Classic CNN	ResNet-18	ResNet-18
Trigger generator model	Autoencoder	Autoencoder	U-Net	Autoencoder
Learning rate of benign task	0.1	0.01	0.01	0.001
Learning rate of backdoor task	0.1	0.01	0.01	0.01
Edge-case	FALSE	TRUE	TRUE	FALSE
Other hyperparameters	Momentum:0.9, Weight Decay: $10^{-4}$			

#### A.4 FTA against other defenses

Besides the defense methods used in the main body, we test the performance of FTA under Multi-Krum, Trimmed-mean, RFA, SignSGD, Foolsgold and SparsedFed. The results prove that FTA is able to evade the defenses.

##### A.4.1 Attack effectiveness under few-shot mode.

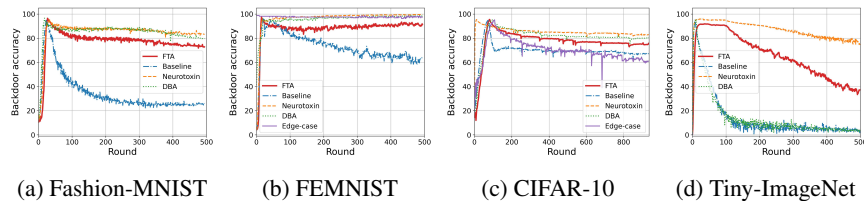


Figure 7: Few-shot attack performance under FedAvg. FTA is more durable than baseline.

The results under few-shot settings are shown in Figure 7. All attacks reach a high BA rapidly after consistently poisoning the server model, then BA gradually drops after stopping attacking and the backdoor injected into the server model is gradually weakened by the aggregation of benign updates. FTA’s performance drops much slower than the baseline attack. For example, in Fashion-MNIST and after 500 rounds, FTA still remains 73% BA, which is only 9% less than Neurotoxin, 61% higher than the baseline. Moreover, FTA can beat DBA and the baseline on Tiny-ImageNet. After 500 rounds, FTA maintains 37% accuracy while the baseline and DBA only have 5%, which is 45% less than Neurotoxin. However, Neurotoxin cannot provide the same stealthiness as shown in following comparison under robust FL defenses. Since malicious and benign updates have a similar direction by FTA, the effectiveness of FTA’s backdoor can survive after few-shot attack. The results prove the durability of FTA.

### A.4.2 Resistance to vector-wise filtering

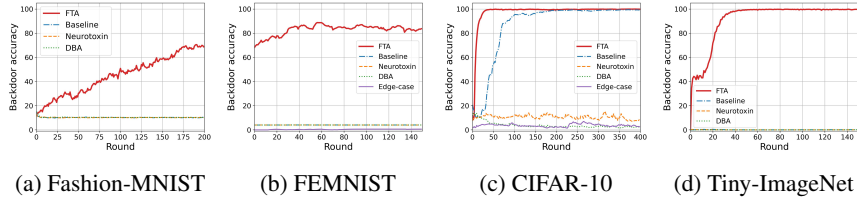


Figure 8: The effectiveness of attack under Multi-Krum in 4 tasks.

Multi-Krum is used as the vector-wise defense method. As described in Appendix A.1.3, it calculates the Euclidean distance between all updates and selects  $n - f - 1$  updates with the smallest Euclidean distances for aggregation. In Figure 8, the defense manages to filter out almost all malicious updates of prior attacks and effectively degrade their attacks’ performance. In contrast, local update of FTA cannot be easily filtered and thus FTA outperforms others. In CIFAR-10 and Tiny-ImageNet, the attack performance is steady for FTA (nearly 100%) within 40 rounds to converge. In FEMNIST, Multi-Krum only results in a 10% BA degradation for FTA while BAs of others are restricted to 0%. In Fashion-MNIST, Multi-Krum can sieve malicious updates of FTA occasionally, leading to a longer convergence time, but still fails to completely defend the FTA. Malicious updates produced by FTA (which successfully eliminates the anomalies in **P1-2**) are with a similar Euclidean distance compared to benign updates, making them more stealthy than other attacks’.

### A.4.3 Resistance to dimension-wise filtering

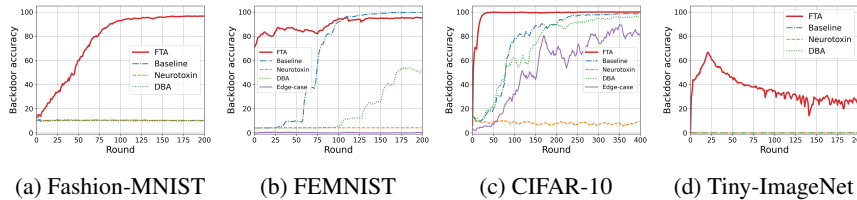


Figure 9: The effectiveness of attack under Trimmed-mean in 4 tasks.

We choose Trimmed-mean as the representative of dimension-wise filtering. As mentioned in Appendix A.1.3, the dimensions of updates are sorted respectively, and the top  $m$  highest and smallest updates are removed, and the arithmetic mean of the rest parameters is computed for aggregated updates. In our experiments,  $m$  is set as 2 because we assume there is no more than one malicious agent during FL iteration, and setting a higher  $m$  can result in lower convergence. As shown in Figure 9, Trimmed-mean successfully filters out the compared attacks in Fashion-MNIST and Tiny-ImageNet, and its effects are weakened in CIFAR-10 and FEMNIST. However, FTA survives in all four tasks and performs the best under trimmed-mean. In CIFAR-10, it completes the convergence within 30 rounds and remains 99.9% BA. In Fashion-MNIST and FEMNIST, FTA takes above 50 rounds to fully converge, and the final accuracy manages to reach 96%. The performance of FTA is significantly degraded in Tiny-ImageNet, but still with 30% advantage over other attacks on average. The update of FTA shares a similar weights/biases distribution of benign updates. This ensures our attack to defeat the defenses based on dimension-wise filtering.

### A.4.4 Resistance to RFA

In Figure 10, FTA provides the best performance among others in Fashion-MNIST, CIFAR-10 and Tiny-ImageNet. In FEMNIST, it converges much faster than prior attacks. Although its accuracy is 8% lower than the baseline in the middle of training, FTA achieves the same performance at the end (of training).

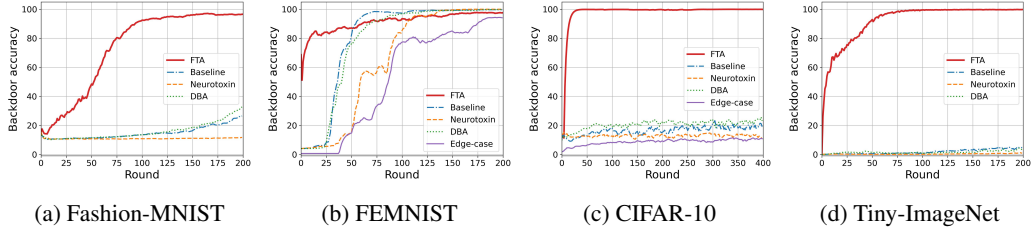


Figure 10: The effectiveness of attack under RFA in 4 tasks.

#### A.4.5 Resistance to SignSGD

As shown in Figure 11 (a)-(b), SignSGD mitigates prior backdoor attacks with a universal trigger pattern. However, FTA still defeats it and remains 94% and 99% BA on Fashion-MNIST and Tiny-ImageNet, respectively.

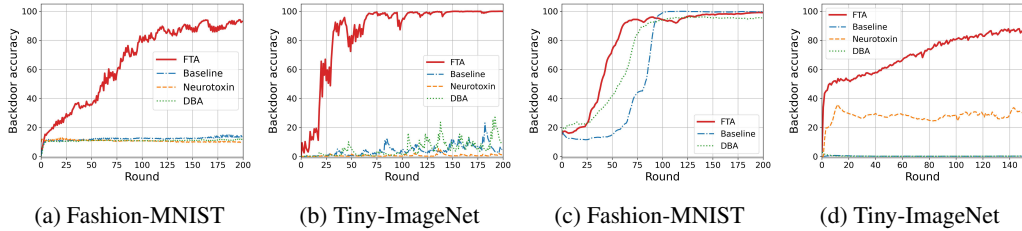


Figure 11: (a)-(b): The effectiveness of attack under SignSGD in Fashion-MNIST and Tiny-ImageNet. (c): The effectiveness of attack under Foolsgold in Fashion-MNIST. (d): The effectiveness of attack under SparseFed in Tiny-ImageNet.

#### A.4.6 Resistance to Foolsgold

From Figure 11 (c), we see that Foolsgold hinders the convergence speed of FTA in Fashion-MNIST, which requires FTA to perform extra 25 rounds for convergence. In this sense, FTA still converges much faster than others.

#### A.4.7 Resistance to sparsification

We choose SparseFed as the representative of the sparsification defense. In Figure 11 (d), only Neurotoxin and FTA are capable of breaking through SparseFed on Tiny-ImageNet. The BA of Neurotoxin exhibits fluctuations (between 22% and 36%) throughout the training process, unable to maintain a continuous rise. In contrast, FTA demonstrates the ability to consistently poison the global model and later achieves an impressive accuracy of 90% by round 150. The reason for the above performance difference is that the backdoor task of FTA captures imperceptible perturbations on model parameters, which eliminates the anomalies of poisoning training. The backdoor tasks trained by FTA are more likely to contribute to the same dimensions of gradients as benign updates. Consequently, the top- $k$  filtering mechanism implemented in the server side is ineffective to filter out FTA’s backdoor effect.

### A.5 Benign accuracy of FTA

We showcase the benign accuracy of both the baseline attack and FTA, and also consider the accuracy without backdoor attacks under FedAvg. We start FTA and the baseline from a specific round (e.g., 0 or 200 for different datasets) and perform the attacks during Attack\_num rounds. We record the accuracy once the attacks have ended. From Table 2, it is evident that FTA results in a slightly smaller decrease in the benign accuracy compared to baseline attack.

Table 2: Benign accuracy of the baseline attack. FTA and no attackers circumstance under different datasets. Benign accuracy drops by  $\leq 1.5\%$  in FTA compared to the accuracy without attack.

Dataset	Attack start epoch	Attack_num	No attack (%)	Baseline attack (%)	FTA (%)
Fashion-MNIST	0	50	90.21	85.14	90.02
FEMNIST	200	50	92.06	91.27	92.05
CIFAR-10	0	100	61.73	56.34	60.61
Tiny-ImageNet	0	100	25.21	19.06	25.13

## A.6 The structure of our models

### A.6.1 The structure of classification models for Fashion-MNIST and FEMNIST

We use an 8-layer classic CNN architecture for training Fashion-MNIST and FEMNIST datasets. The details are shown in Table 3.

Table 3: The structure of classic CNN model.

Parameters	Shape	Hyperparameters of layer
Conv2d	1*32*3*3	stride = (1, 1)
GroupNorm	32*32	eps = $10^{-5}$
Conv2d	32*64*3*3	stride = (1, 1)
GroupNorm	32*64	eps = $10^{-5}$
Dropout2d		p = 0.25
Linear	9216*128	bias = True
Linear(For Fashion-MNIST)	128*10	bias = True
Linear(For FEMNIST)	128*62	bias = True

### A.6.2 The structure of trigger generator

In the FTA framework, the trigger generator plays a crucial role in feature extraction in the sense that it aims to align the hidden features of poisoned samples with the target label samples. We utilize the Autoencoder as the trigger generator due to its ability to capture essential features of input and generate outputs satisfying our needs. Moreover, we find that U-Net exhibits comparable performance for trigger generation while requiring less training data, as stated in [15]. Therefore, we include U-Net in our experiments. Both U-Net and autoencoder architectures used to train the trigger generator  $g_\xi$  are similar to those presented in [15].

### A.6.3 The structure of classification models for CIFAR-10 and Tiny-ImageNet

We use a similar ResNet-18 architecture as in [55] for training CIFAR-10 and Tiny-ImageNet.

## A.7 Other experiment settings

The implementation of all the compared attacks and FL framework are based on PyTorch [37]. We test the experiments on a server with one Intel Xeon E5-2620 CPU and one NVIDIA A40 GPU with 32G RAM.

In Fashion-MNIST, CIFAR-10 and Tiny-ImageNet, a Dirichlet distribution is used to divide training data for the number of total agent parties, and the hyperparameter for distribution is 0.7 for the datasets. For FEMNIST, we randomly choose data of 3000 users from the dataset and randomly distribute every training agent with the training data from 3 users. All parties use SGD as an optimizer and train for local training epochs with a batch size of 256. A global training model is shared by all agents, and updates of 10 agents will be selected for aggregating the global model. Benign agents train with

a benign learning rate for benign epochs. The attacker’s local training dataset is mixed with 80% correct labeled data and 20% poisoned data. The target labels are “sneaker” in Fashion-MNIST, “digit 1” in FEMNIST, “truck” in CIFAR-10 and “tree frog” in Tiny-ImageNet. The attacker has its own local malicious learning rate and epochs to maximize its backdoor performance. It also needs to train its local trigger generator with learning rate and epochs before performing local malicious training on the downloaded global model.

Regarding the attack methods, we set the top- $k$  ratio of 0.95 for Neurotoxin, in line with the recommended settings in [62]. For DBA, we use 4 distributed strips as backdoor trigger patterns. Both the baseline attack and Neurotoxin employ a “square” trigger pattern on the top left as the backdoor trigger. We conduct Edge-case attack on CIFAR-10 and FEMNIST. Specifically, for CIFAR-10, we use the southwest airplane as the backdoored images and set the target label as “bird”. For FEMNIST, we use images of “7” in ARDIS [23] as poisoned samples with the target label set as the digit “1”. The dataset settings of the experiments are the same as those used in [48].

### A.7.1 Visualization of different trigger sizes

The benign and poisoned samples with flexible triggers of different sizes generated by FTA are presented in Figure 12. For Tiny-ImageNet and CIFAR-10, it is hard for human inspection to immediately identify the triggers, which proves the stealthiness in P3. In Fashion-MNIST and FEMNIST, the triggers are easier to distinguish because there is only one channel of the input samples in the datasets. But those flexible triggers are still much more stealthy compared to those produced by prior attacks on FL (see Figure 2).

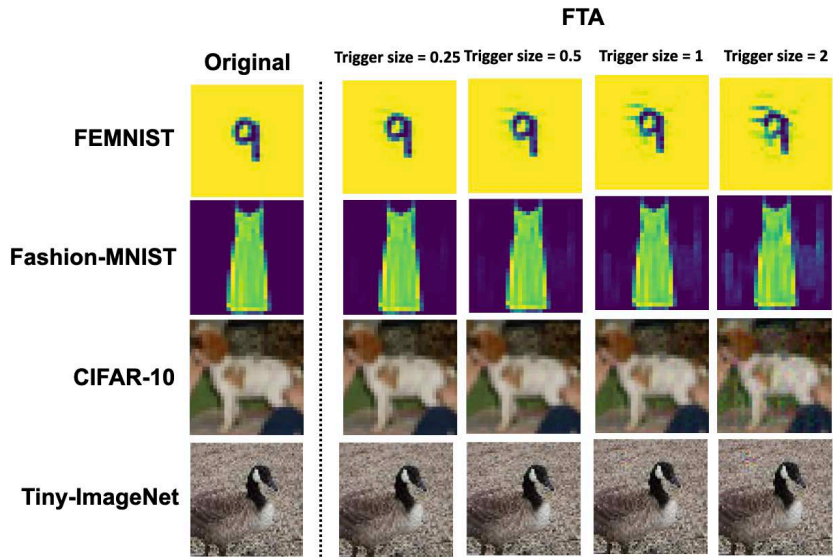


Figure 12: Visualization of backdoored images of different trigger sizes.

### A.8 Other ablation studies in FTA attack

**Poison Fraction.** We set the local training batch size to 256 for all the tasks, follow the standard settings of other FL frameworks, and set the poison fraction as 0.2. As stated in Appendix A.5, this fraction setting cannot degrade the performance of benign accuracy and meanwhile, we would like to explore further to examine the lower bound of the fraction which FTA’s performance can tolerate. In Figure 13 (a)-(d), FTA is still effective whilst the fraction drops to 0.05. We also find that sensitivities to poison fraction can vary among tasks. In Fashion-MNIST and CIFAR-10, FTA remains its performance even if poison fraction = 0.01, in which only 3 samples are poisoned in each batch. As for FEMNIST and Tiny-ImageNet, under the same rate, the backdoor tasks are dramatically weakened by the benign ones.

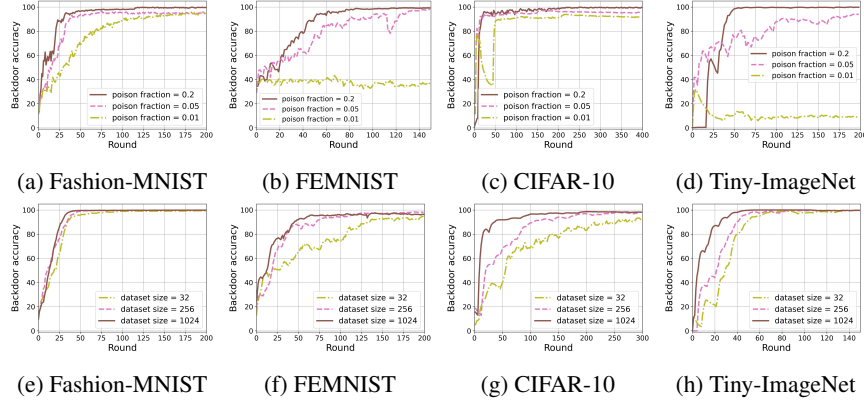


Figure 13: Different hyperparameters on backdoor accuracy. (a)-(d): poison fraction; (e)-(h): dataset size of trigger generator.

Table 4: Experimental results on trigger stealthiness (SSIM $\uparrow$  and LPIPS $\downarrow$ ).

Dataset	Metric	Baseline	DBA	Neurotoxin	Edge-case	FTA(Ours)
Fashion-MNIST	SSIM	0.9376	0.9052	0.9359	-	<b>0.9967</b>
	LPIPS	NA	NA	NA	NA	NA
CIFAR-10	SSIM	0.9612	0.9440	0.9638	0.7354	<b>0.9978</b>
	LPIPS	0.0058	0.0091	0.0075	0.3171	<b>0.0008</b>
Tiny-ImageNet	SSIM	0.9851	0.9734	0.9810	-	<b>0.9881</b>
	LPIPS	0.0072	0.0149	0.0086	-	<b>0.0029</b>

**Dataset Size of Trigger Generator.** During the training, if the attacker controls multiple agents, it can merge all local datasets into one for generator training. However, in many cases, the attacker can only control relatively limited agents and is provided by a small-scale dataset for training. Recall that in Algorithm 1 we use the same dataset for the malicious classification model and trigger generator training. We set the size of dataset for learning trigger generator to 1024 for all tasks in default. Even if the size of the dataset is only set to 32, FTA can provide a high attack performance (see Figure 13 (e)-(h)). We note that the training process here is somewhat similar to generative adversarial networks, in which we do not require a large amount of samples in the training dataset.

## A.9 Natural stealthiness

For each dataset, we randomly select 500 sample images from test dataset to evaluate the trigger stealthiness. As the SSIM value increases, the poisoned sample looks more stealthy. But for LPIPS, that is the other way round. Table 4 shows that FTA achieves excellent stealthiness in all cases. Specifically, SSIM values of FTA are the highest in these datasets, which are close to 1. LPIPS values of FTA are 2-7 $\times$  improvement to that of baseline attack. Although the baseline attack and Neurotoxin, which uses a universal square pattern, performs well on more complex datasets, using such a patch-based pattern can make the original image look “unnatural”.

Table 5: Time consumption and computational cost (MEAN $\pm$ SD) of different attack methods in one FL iteration under Fashion-MNIST, CIFAR-10 and Tiny-ImageNet.

Dataset $\rightarrow$	Fashion-MNIST		CIFAR-10		Tiny-ImageNet	
Attack $\downarrow$	Time (s)	Memories (MB)	Time (s)	Memories (MB)	Time (s)	Memories (MB)
Benign	1.62 $\pm$ 0.19	76.8	14.11 $\pm$ 1.45	125.1	37.92 $\pm$ 2.71	233.5
Baseline Attack	1.67 $\pm$ 0.25	81.6	14.81 $\pm$ 2.10	127.2	38.52 $\pm$ 2.19	226.4
DBA	1.57 $\pm$ 0.31	81.7	14.91 $\pm$ 1.86	124.7	38.74 $\pm$ 1.92	248.5
Neurotoxin	3.39 $\pm$ 0.66	120.4	27.85 $\pm$ 1.74	279.3	76.38 $\pm$ 3.46	478.7
FTA	2.04 $\pm$ 0.52	86	18.38 $\pm$ 1.89	169.1	46.98 $\pm$ 2.14	298.4

## A.10 Computational cost

We understand the significance of the external computational cost and time consumption of backdoor training on malicious devices in our proposed attack under FL scenario. Training with GANs in federated systems introduces extra time consumption. However, our attack does not significantly increase the computational and time cost due to our optimization procedure. Compared to training benign task and baseline backdoor task, FTA only needs to train an additional trigger generator which is actually a small generative neural network. Our generator only consists of several convolutional layers in total. It is worth noting that the datasets used to train both two network structures comprise only 1024 poisoned samples as shown in Table 1 whose size are relatively small compared to the entire training dataset. For instance, the training dataset for our trigger generator accounts for approximately 0.14% of the FEMNIST dataset. Therefore, the time consumption and computational cost for training this generative network are very minimal. The remaining time consumption is comparable to training a benign local model. As shown in Table 5, Neurotoxin requires approximately  $2\times$  the time and memory compared to benign training to complete backdoor training for one FL round. This is attributed to an additional local benign training requirement in Neurotoxin. However, FTA consumes less than 30% additional time and 25% additional computational cost for backdoor training compared to benign ones. Given that FTA remains under 70% of the cost of Neurotoxin, it is practical to conduct an FTA attack in decentralized scenario.

## A.11 Discussion

In this work, we concentrate on the computer vision tasks, which have been the focus of numerous existing works [55, 48, 15, 64, 35]. In the future, we intend to expand the scope of this work by applying our design to other real-world applications, such as natural language processing (NLP) and reinforcement learning (RL), as well as other vision tasks, e.g., object detection.

The primary focus of FTA is to achieve stealthiness rather than durability, in contrast to other attacks such as Neurotoxin [62]. Neurotoxin manipulates malicious parameters based on gradients in magnitude, which yields a clear increase in the dissimilarity of parameters and thus harms the stealthiness of the attack. FTA addresses the dissimilarity difference of weights/biases introduced by backdoor training by using a stealthy and adaptive trigger generator, which makes the hidden features of poisoned samples similar to benign ones. We emphasize that the durability of backdoor attacks on FL is orthogonal to the main focus of this work, and we leave it as an open problem. A possible solution to achieve persistence could be to decelerate the learning rate of malicious agents, as proposed in [2].

**Comparison.** In addition to the defenses evaluated in this paper, we discuss our attack effectiveness under other defenses below. As depicted in FLDetector [61], in a typical FL scenario where the server does not have a validation dataset that Fltrust [8] requires, the global model remains susceptible to backdoor attacks. However, the stringent demand by Fltrust for an extra validation dataset could not be practical for conventional FL frameworks and applications. Furthermore, Fltrust eliminates backdoor effectiveness based on cosine dissimilarity which is similar to the approach used in FLAME. As shown in Figure 5, FTA’s malicious updates have less dissimilarity to benign updates than the baseline attack’s. Therefore, we can state that FTA can evade Fltrust according to the results obtained under FLAME. DnC [42] primarily focuses on untargeted poisoning attacks rather than backdoor attacks, and its main objective is to reduce the accuracy of FL models. Accordingly, we do not consider it as a “proper” SOTA backdoor defense (to our attack). In particular, DnC is a kind of vector-wise filtering defense. In our experiments, conducted under Multi-krum and RFA, we ascertain that FTA is robust against vector-wise filtering. In conclusion, FTA can also successfully evade DnC, much like Multi-krum and RFA. As for certified defense like Flcert [9], while it is a promising approach to robustness certification, it is not intended to detect and filter out malicious updates in FL. As outlined in Flcert, the certified accuracy of the global model experiences a decline with the increase of malicious agents. Fortunately, FTA can cope with a very challenging threat model, where the attacker is allowed to control merely one malicious agent out of thousands. We thus can achieve a certified accuracy almost on par with the original global model accuracy against Flcert. FLIP [59] only considers static backdoors as potential attacks, i.e. patch-based patterns, whereas FTA can use flexible triggers to break FLIP’s threat model. Using the flexible trigger generator, FTA can produce sample-specific triggers which pose challenges when applying universal trigger inversion method in FLIP’s step 1.